

Combined Cyclin D1 Overexpression and Zinc Deficiency Disrupts Cell Cycle and Accelerates Mouse Forestomach Carcinogenesis¹

Louise Y. Y. Fong, Rita Mancini, Hiroshi Nakagawa, Anil K. Rustgi, and Kay Huebner²

Kimmel Cancer Center, Jefferson Medical College, Thomas Jefferson University, Philadelphia, Pennsylvania 19107 [L. Y. Y. F., R. M., K. H.], and Division of Gastroenterology, Department of Genetics, Cancer Center, Abramson Family Cancer Research Institute, University of Pennsylvania, Philadelphia, Pennsylvania 19104 [H. N., A. K. R.]

ABSTRACT

Overexpression of cyclin D1 and disruption of cell cycle control in G₁ occur frequently in human esophageal cancer. Transgenic (TG) mice with cyclin D1 overexpression targeted to the oral-esophageal tissue by the EBV ED-L2 promoter showed increased severity in esophageal dysplasia without cancer development, after multiple doses of *N*-nitrosomethylbenzylamine (NMBA). Dietary zinc deficiency (ZD) in mice enhances cellular proliferation in esophagus/forestomach and susceptibility to NMBA-induced carcinogenesis. We investigated whether cyclin D1 overexpression in TG mice, together with ZD, might lead to unchecked cell proliferation and accelerated NMBA-induced tumorigenesis. Five-week-old TG and wild-type (WT) mice were fed a ZD- or -sufficient (ZS) diet, forming four groups: ZD:TG; ZS:TG; ZD:WT; and ZS:WT. After 4 weeks, animals were given a single intragastric NMBA dose and were sacrificed 25 and 77 days later. Without NMBA, cell proliferation was greatest in ZD:TG esophagus/forestomach, followed by ZD:WT, and then ZS:TG ≥ ZS:WT. The high rate of cell proliferation was accompanied by overexpression of cell cycle progression and tumorigenesis biomarkers, including proliferating cell nuclear antigen, cyclin D1, cyclin-dependent kinase 4, p53, cytokeratin 14, epidermal growth factor receptor, and by a reduced rate of apoptosis. ZD substantially increased forestomach tumor incidence in TG mice: 85% of ZD:TG versus 14% of ZS:TG mice had forestomach tumors ($P < 0.001$), with progression to malignancy occurring only in ZD:TG tumors. Additionally, 14% of ZD:TG mice developed esophageal tumors and esophageal intestinal metaplasia at 77 days. Thus, cyclin D1 overexpression, in cooperation with ZD, decontrols cell proliferation, ensuring cell expansion, a prerequisite for cancer development.

INTRODUCTION

ESCC³ shows wide variations in geographical distribution and incidence (1). Although alcohol and tobacco consumption are major risk factors in industrialized countries, other factors such as nutritional deficiencies, including that of zinc (2–4), and environmental exposure to *N*-nitrosamines, including NMBA (3, 5, 6), play an important role in the pathogenesis of this disease worldwide.

The sequence of histopathological changes in ESCC development typically involves hyperplasia, mild to severe dysplasia, carcinoma *in situ*, and, finally, invasive carcinoma. Genetic steps that accompany such changes frequently include mutation of the *TP53* tumor suppressor gene, disruption of cell cycle control in G₁ involving the p16^{ink4a}-cyclin D1/Cdk4-Rb pathway, activation of oncogenes such as *EGFR*,

and inactivation of several tumor suppressor genes (7). Notably, cyclin D1 overexpression because of gene amplification is a critical genetic alteration in ESCC (8, 9) and in Barrett's esophagus, a premalignant condition of esophageal adenocarcinoma (10). Overexpression of cyclin D1 has been reported in esophageal papillomas and carcinomas isolated from rats at end point after multiple exposures to NMBA (11, 12), providing evidence that overexpression of cyclin D1 is also fundamental to the process of esophageal carcinogenesis in animal models.

Nakagawa *et al.* (13) developed a TG mouse in which the EBV ED-L2 promoter targets the transgene to the stratified squamous epithelium of tongue, esophagus, and forestomach, resulting in a dysplastic phenotype associated with increased cell proliferation (14). However, TG mice, exposed to multiple doses of NMBA, showed increased severity of esophageal dysplasia after 12–15 months, indicating that cyclin D1 overexpression was not sufficient to elicit a tumorigenic response to induction by NMBA (15), the most widely used agent for esophageal tumor induction in rodents (16).

Our ZD-NMBA rat esophageal cancer model is an important tool to study molecular mechanism(s) underlying ESCC cancer development and prevention (17–23). In this model, tumorigenesis is driven by increased cell proliferation, created in the esophageal epithelium by dietary ZD (18); thus, a single nontumorigenic NMBA dose (24) elicits an 80–95% tumor incidence in ZD esophagus after 12 weeks (19–23). Tumor initiation (20) and reversal (23) is extremely rapid in ZD esophagus, allowing quasi-synchronous cellular responses to such processes to be precisely delineated. For example, 24 h after NMBA treatment, there was an expansion in the size of focal hyperplastic lesions in ZD esophageal epithelium, with abundant PCNA-positive cells. Adjacent sections displayed concurrent increases in cyclin D1, Cdk4, Rb expression, and reduced p16^{ink4a} staining (20), demonstrating a link between deregulation of the p16^{ink4a}-cyclin D1/Cdk4-Rb pathway that regulates G₁-S progression and rapid initiation of esophageal tumors.

ZD mice also develop tumors readily in response to NMBA (25, 26), with a lower incidence of esophageal than forestomach tumors; the rodent forestomach is considered as an extension of the lower esophagus (25). Given that cyclin D1 overexpression (13–15) and dietary ZD (25, 26) in mice are both connected with a high rate of esophageal/forestomach cell proliferation, we postulated that in combination, they may additionally deregulate cell cycle progression, thereby predisposing TG mice fed a ZD diet to NMBA-induced carcinogenesis.

MATERIALS AND METHODS

Chemicals and Animal Diets. NMBA was from Ash Stevens, Inc. (Detroit, MI). Custom-formulated, egg white-based, ZD and ZS diets were prepared by Teklad (Madison, WI). The two diets were identical except for the amount of zinc carbonate, which was 1.5 ppm for the ZD diet and 74–75 ppm for the ZS diet. Zinc levels in these diets were monitored regularly by atomic absorption spectroscopy.

Transgenic Mice. The generation of TG mice was described previously (13). Breeding of TG males from a single founder line to B6 females generated a total of 65 TG mice for the tumorigenesis study. TG offspring were analyzed

Received 3/14/03; accepted 5/6/03.

The costs of publication of this article were defrayed in part by the payment of page charges. This article must therefore be hereby marked *advertisement* in accordance with 18 U.S.C. Section 1734 solely to indicate this fact.

¹ This work was supported by American Institute for Cancer Research Grant 02A025-REN (to L. Y. Y. F.), the Italian-American Cancer Foundation Fellowship (to R. M.), NIH Grants DK3377 (to A. K. R.) and NIH P01 DE12467 (to A. K. R.), and by National Cancer Institute Grants CA77738 (to K. H.) and CA53036.

² To whom requests for reprints should be addressed, at Thomas Jefferson University, Jefferson Medical College, Kimmel Cancer Institute, 233 South 10th Street, Philadelphia, PA 19107-6799. Phone: (215) 503-4656; Fax: (215) 923-3528.

³ The abbreviations used are: ESCC, esophageal squamous cell carcinoma; TG, cyclin D1 transgenic; WT, wild-type; ZD, zinc deficient; ZS, zinc sufficient; NMBA, *N*-nitrosomethylbenzylamine; Cdk, cyclin-dependent kinase; Rb, retinoblastoma; B6, C57BL/6; SCJ, squamocolumnar junction between fore- and hindstomach; PCNA, proliferating cell nuclear antigen; EGFR, epidermal growth factor receptor; ISOL, *in situ* oligo ligation method; LI, labeling index; AZ, antizyme; DAB, 3,3'-diaminobenzidine tetrahydrochloride.

for presence of the transgene by genotyping of tail DNA using a PCR amplification method (13). WT B6 male mice were obtained from Jackson Laboratory (Bar Harbor, ME).

Experimental Design. This study was approved by the Thomas Jefferson University Institutional Animal Care and Use Committee and conducted under NIH guidelines. Briefly, 4–5-week-old mice were randomized into two dietary groups and were fed *ad libitum* with a ZD or ZS diet and given free access to deionized drinking water, thus forming four experimental groups, ZD:TG, ZS:TG, ZD:WT, and ZS:WT. After 5 weeks, 7 mice from each group were sacrificed to determine the effect of dietary ZD on the extent of cell proliferation in the esophagus/forestomach. The remaining mice (10–14/group) received a single NMBA dose at 2 mg/kg body weight. At 25 days after NMBA treatment, a moribund ZD:TG mouse was autopsied and was found to harbor large fused tumors in the forestomach. Thus, we sacrificed half the transgenic mice at 25 days, and the remaining at 77 days for end point tumor incidence analysis.

Zinc Determination. At autopsy, testis from male mice and hair from female mice were dried to constant weights at 90°C and ashed in a furnace. Ashed samples were dissolved in 0.1 N HCl and zinc levels determined by atomic spectrometry (26), using a Perkin-Elmer Atomic Absorption Spectrometer Analyst 100 (Perkin-Elmer, Norwalk, CT). Zinc content was expressed as $\mu\text{g/g}$ dry weight. Zinc content in the testis (male) and hair (female) was significantly lower in ZD than ZS mice, independent of genotype or NMBA treatment. For example, in NMBA-untreated mice, testis and hair zinc content were significantly lower in ZD:TG versus ZS:TG mice (testis, 115 ± 10 versus 151 ± 6 $\mu\text{g/g}$; hair, 132 ± 12 and 189 ± 15 $\mu\text{g/g}$, $P < 0.001$), in agreement with previous studies (26).

Tumor Analysis. At sacrifice, the animals were subjected to complete autopsies. Whole stomach and esophagus were excised and opened longitudinally. Tumors > 0.5 mm in diameter in the esophagus/forestomach were counted.

Isolation of Forestomach Tissue. Whole esophagus/forestomachs were fixed in buffered formalin and embedded in paraffin. Cross-sections of the forestomach, including SCJ, were cut 4- μm thick. Serial sections were prepared and stained with H&E for histopathology or left unstained for immunohistochemical studies.

Cell Proliferation Determination by PCNA Immunohistochemistry. Monoclonal mouse anti-PCNA (Santa Cruz Biotechnology, Santa Cruz, CA) was used at 1:500 dilution, followed by incubations with biotinylated goat antimouse antibody and streptavidin horseradish peroxidase. PCNA was localized by incubation with 3-amino-9-ethylcarbazole-substrate-chromogen system (Dako Corp.) and a light hematoxylin counterstain. Cells with red reaction product in the nucleus were considered positive for the presence of PCNA.

Immunohistochemical Detection of Cyclin D1, Cdk4, p53, Cytokeratin, EGFR, Bax, and Bcl-2. After deparaffinization and rehydration in graded alcohols, sections were heated in citrate buffer (0.01 M, pH 6.0) in a microwave oven (85–90°C, 3 \times 5 min) before nonspecific binding sites were blocked with goat/rabbit serum. Sections were incubated overnight at 37°C in a humidified chamber with respective primary antibodies: rabbit anticyclin D1 polyclonal antibody (Lab Vision Corp., Fremont, CA) at 1:100 dilution; rabbit anti-Cdk4 polyclonal antibody (Santa Cruz Biotechnology) at 1:150 dilution; rabbit anti-p53 polyclonal antibody (Novocastra Lab., Newcastle upon Tyne, United Kingdom) at 1:250; mouse anticytokeratin 14 monoclonal antiserum (Clone LL002; Novocastra Lab.) at a 1:40 dilution, goat anti-EGFR polyclonal antibody (Santa Cruz Biotechnology) at 1:60 dilution; rabbit anti-Bcl-2 polyclonal antiserum (Santa Cruz Biotechnology) at a 1:3000 dilution, and rabbit anti-Bax polyclonal antiserum (Santa Cruz Biotechnology) at a 1:800 dilution. Incubation with appropriate biotinylated secondary antibodies followed. Slides were then incubated with streptavidin horseradish peroxidase, and expression of individual proteins was localized by incubation with DAB and a light hematoxylin counterstain. The cyclin D1 monoclonal antibody used has no cross-reactivity with cyclin D2 or D3, and Cdk4 polyclonal antibody has no cross-reactivity with other Cdk.

Bcl-2:Bax Ratio. The Bcl-2:Bax ratio was obtained by dividing the immunoreactive score of Bcl-2 by that of Bax. An immunoreactive score was calculated by multiplying the grade of percentage of positive cells by that of intensity of staining (27). The percentage of Bax- or Bcl-2-positive cells was graded semiquantitatively as follows: 0 = 0–5%; 1 = 6–25%; 2 = 26–50%;

3 = 51–75%; and 4 = 76–100%; the intensity of staining was graded as follows: 0 = none; 1 = weak; 2 = moderate; and 3 = intense. When heterogeneous staining intensities were found within one forestomach section, each component was graded independently, and the results were summed. For example, a specimen that contained 50% of cells with moderate intensity ($2 \times 2 = 4$), 25% of cells with intense immunostaining ($1 \times 3 = 3$), and 25% of cells with no staining ($1 \times 0 = 0$) would receive an immunoreactive score $7 (4 + 3 + 0 = 7)$.

Apoptosis Detection. Apoptosis was assessed by the ISOL method that uses T4 DNA ligase to specifically join DNase I-type ends from genomic DNA in the sample to biotin-labeled hairpin oligonucleotide probes (28, 29). These probes specifically and sensitively detect double-strand breaks in apoptotic cells. Although conventional *in situ* detection techniques such as terminal deoxynucleotidyl transferase-mediated nick end labeling are useful in detecting internucleosomal DNA cleavage, they do not differentiate DNase I-type cleavage, which results from the activation of apoptotic endonucleases. Thus, the ISOL method is more selective in avoiding labeling of randomly damaged DNA.

ISOL Assay. The double-strand breaks in DNA in apoptotic cells were detected using an ApopTag ISOL kit (Serological Corp., Norcross, GA). Briefly, the sections were deparaffinized, rehydrated in a graded alcohol series, and incubated with proteinase K. Endogenous peroxidase in the sections was inhibited with 3% hydrogen peroxide. The slides were then incubated with T4 DNA ligase enzyme to catalyze blunt end ligation of biotinylated Oligo B (blunt end oligo) and fragmented double-strand DNA (16°C–20°C for 17 h). Next, the slides were incubated with streptavidin peroxidase, and DNA fragmentation was detected by staining with DAB. Finally, the sections were counterstained with methyl green. Sections from rat mammary gland in which extensive apoptosis occurs served as a positive control. Negative controls omitted T4 DNA ligase enzyme.

Statistical Analysis. Data on cell proliferation were analyzed by one-way ANOVA with the SAS statistical computer program (30). Tumor incidence differences were analyzed by two-tailed Fisher's exact test (31). All statistical tests were two-sided and were considered statistically significant at $P < 0.05$.

RESULTS

Macroscopic Lesions in Untreated ZD:TG Forestomach. Transgenic ZD:TG mice on a ZD diet for 5 weeks showed thickened forestomachs and esophagi, with 2 of 7 animals displaying conspicuous lesions in the forestomach and SCJ (Fig. 1A, b). By contrast, transgenic ZS:TG mice on ZS diet, showed thin forestomach epithelia and slightly thickened SCJs (Fig. 1A, a), resembling ZS:WT forestomachs (data not shown; Ref. 26), whereas, ZD:WT forestomachs exhibited thickened mucosa (data not shown; Ref. 26). The forestomach/esophagus thickening was greatest in ZD:TG mice, followed by ZD:WT and then ZS:TG \geq ZS:WT. These results indicate that cyclin D1 overexpression in TG mice, together with dietary ZD, produced greater thickening in forestomach than observed with either condition alone, suggesting the combination led to unbridled cell proliferation.

Rapid Induction and Progression of Forestomach Tumors in NMBA-treated ZD:TG Mice. Table 1 shows that as early as 25 days after a single NMBA dose, 85% (11 of 13) of ZD:TG mice developed tumors in forestomach/SCJ, with 46% showing fused tumors, often occupying the entire forestomach (Fig. 1A, d) and 39% with large individual tumors (1.5–2.5 mm in diameter). Conversely, 86% (12 of 14) of ZS:TG mice were tumor-free (Fig. 1A, c), and 14% (2 of 14) had very small forestomach tumors (< 1 mm in diameter, data not shown), a result at variance with a previous study in which NMBA-exposed TG mice without zinc restriction developed dysplasia without cancer (15). This variation is probably attributable to a difference in the route of administration of NMBA, *s.c.* versus intragastric administration in this study. There was no increase in tumor incidence in either group when the end point was extended to 77 days (Table 1). At both 25 and 77 days, ZD:TG mice had significantly higher tumor incidence than ZS:TG mice ($P < 0.001$), indicating that ZD increases the incidence of tumors in transgenic mice overexpressing cyclin D1.

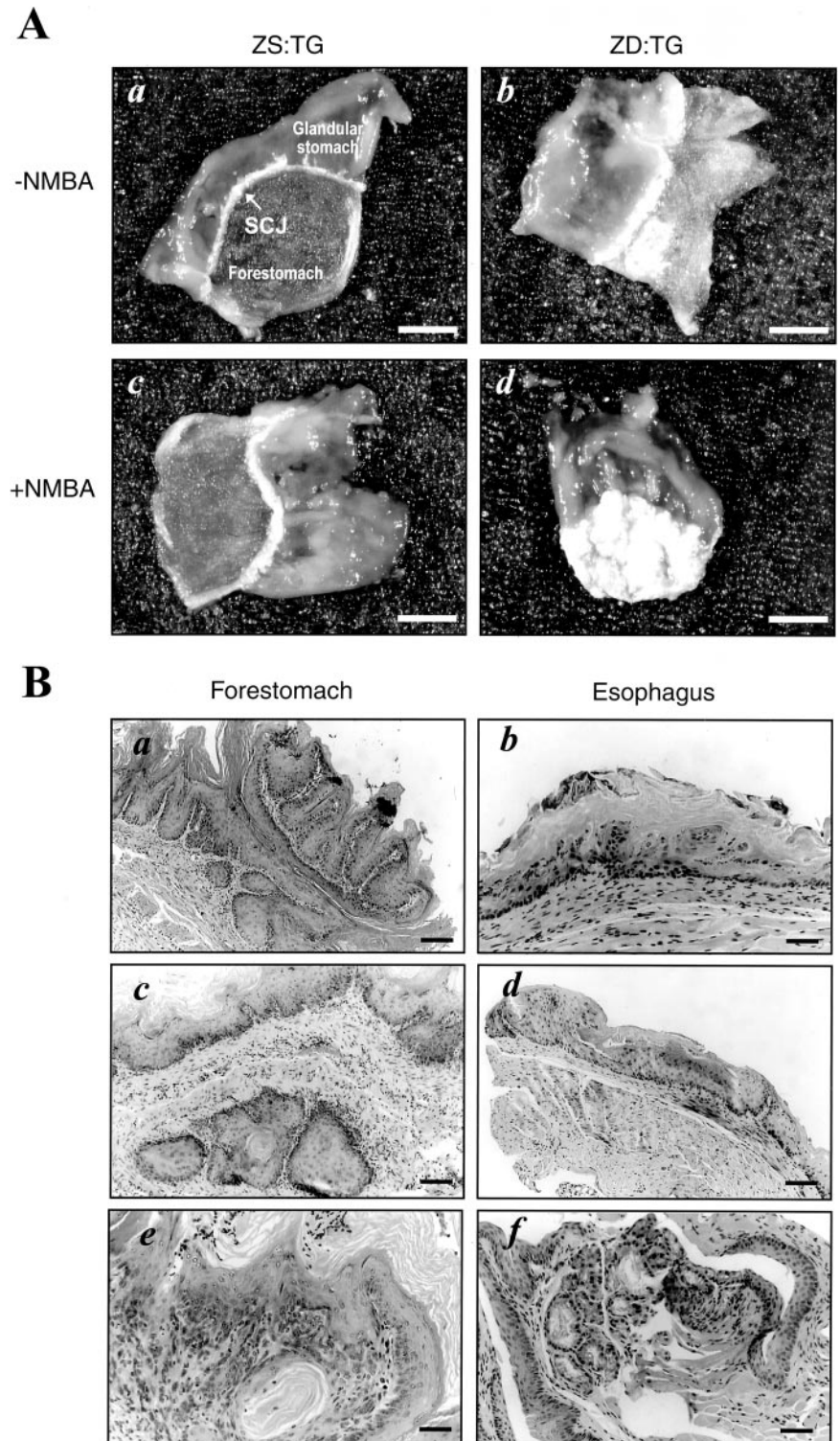


Fig. 1. *A*, macroscopic and microscopic views of forestomachs of ZD:TG mouse forestomachs with and without ZD diet and NMBA treatment. *a* and *b* (-NMBA), ZS:TG mouse 8 shows a normal forestomach with a slightly thickened SCJ (*a*) versus ZD:TG mouse 1 exhibiting a thickened forestomach mucosa and SCJ, with a patch of thickening in forestomach (*b*). *c* and *d* (+NMBA, 25 days), ZD:TG mouse exhibits large fused tumors in forestomach/SCJ (*d*) versus ZS:TG mouse showing a tumor-free forestomach with a thickened SCJ (*c*). Scale bar = 3.5 mm. *B*, forestomach and esophageal microscopic lesions in ZD:TG mice 25 and 77 days after a single NMBA dose. H&E-stained sections. *a*, squamous cell papilloma of the forestomach (mouse 33, 25 days). *c*, endophytic squamous cell carcinoma of the forestomach (mouse 20, 25 days). *e*, squamous cell carcinoma of the forestomach (forestomach (mouse 34, 77 days). *b*, early papilloma in esophagus (mouse 20, 25 days). *d*, focal hyperplastic lesions in esophagus (mouse 19, 25 days). *f*, glandular metaplasia in esophagus (mouse 38, 25 days). Scale bar = 50 μm.

On the other hand, a single NMBA dose induced very small forestomach tumors in 20% (2 of 10) of ZD:WT at 77 days but 0% (0 of 10) of ZS:WT mice; the difference was not statistically significant. The lack of effect of ZD on forestomach tumorigenesis in WT mice is attributable to the single rather than multiple NMBA doses (25). Notably, there was a significant difference in forestomach tumor incidence between transgenic mice on a ZD diet (ZD:TG versus ZD:WT, $P = 0.003$) but not those on a ZS diet (Table 1). These results suggest that the accelerated and enhanced NMBA-induced fore-

stomach tumorigenesis observed in ZD:TG mice was driven by joint efforts of ZD and cyclin D1 overexpression.

Histopathological analysis of ZD:TG forestomach sections revealed an array of lesions, including deep downward focal hyperplasia, dysplasia, papillomas (Fig. 1B, *a*), and squamous cell carcinomas (Fig. 1B, *c* and *e*). Conversely, ZS:TG forestomach exhibited mostly hyperplasia, with infrequent occurrence of dysplasia and papillomas (data not shown). These results are consistent with the tumorigenesis data presented for these two groups of animals in Table 1. In addition,

Table 1 Rapid induction of forestomach tumors in ZD:TG mice by a single NMBA dose

Diet:genotype	Days after NMBA treatment	Tumor incidence (%) ^a		Forestomach tumor size % of mice ^b		
		Esophagus	Forestomach/SCJ ^c	Fused	Large	Small
ZD:TG	25	1/13 (8)	11/13 (85)	46	39	0
ZS:TG	25	0/14 (0)	2/14 (14)	0	0	14
ZD:TG	77	2/14 (14)	12/14 (86)	50	36	0
ZS:TG	77	0/10 (0)	1/10 (10)	0	0	10
ZD:WT	77	0/10 (0)	2/10 (20)	0	0	20
ZS:WT	77	0/10 (0)	0/10 (0)	0	0	0

^a Tumor incidence (number of mice with tumors/total number of mice) was analyzed by Fisher's exact test, two-tailed.

^b Tumor size: fused, numerous tumors fused together, occupying the entire forestomach or an area >3 × 4 mm; large, tumors 1.5–2.5 mm in diameter; small, tumors <1 mm in diameter.

^c SCJ, SCJ with the glandular stomach. Effect of ZD on tumor incidence: ZD:TG versus ZS:TG, forestomach/SCJ, $P < 0.001$ (25, 77 days). Effect of cyclin D1 overexpression on tumor incidence: ZD:TG versus ZD:WT, forestomach/SCJ, $P = 0.003$ (77 days). All statistical tests were two-sided.

ZD:TG mice had significantly higher incidence of forestomach squamous cell carcinomas than ZS:TG animals at both end points [4 of 13 (31%) versus 0 of 14 (0%) at 25 days, $P = 0.04$; and 5 of 14 (36%) versus 0 of 10 (0%) at 77 days, $P = 0.05$]. These data showed that in the ZD condition, tumor progression to malignancy was very rapid in TG mice.

Esophageal Lesions in NMBA-treated ZD:TG Mice. Macroscopic esophageal lesions were not detected in ZD:WT mice after a single NMBA dose, a result consistent with our previous reports that, unlike the rat, mouse esophagus is less sensitive to NMBA carcinogenicity than forestomach (25, 26). However, small esophageal tumors were detected in 8% (1 of 13) and 14% (2 of 14) of ZD:TG mice at 25 and 77 days, respectively, but not in ZS:TG mice ($P > 0.05$). H&E-stained sections of ZD:TG esophagi typically showed the occurrence of a thickened epithelium with focal hyperplastic lesions (Fig. 1*B, d*). An example of an early papilloma is shown in Fig. 1*B, b*. In addition, esophageal intestinal metaplasia was detected in 2 ZD:TG mice, 1 at 25 days (Fig. 1*B, f*) and the other 77 days (data not shown). By contrast, esophagi from ZS:TG mice at both end points exhibited none of these lesions, and ZS:TG esophageal epithelia were typically 2–5 cells thick with mild to moderate basal cell hyperplasia (data not shown).

Unchecked Cell Proliferation in Untreated ZD:TG Forestomach. We determined whether a combination of cyclin D1 overexpression in TG mice and ZD resulted in greater abnormalities in cell cycle-related proteins than observed with either condition alone. We accomplished this by immunohistochemical analyses to compare the expression of relevant biomarkers, including PCNA, cyclin D1, Cdk4, p53, EGFR, and cytokeratin 14 [an important biomarker of cell differentiation in esophageal carcinogenesis (26, 32)], in the forestomach of ZS:TG versus ZD:TG mice and in control ZS:WT and ZD:WT animals. We present detailed results from TG forestomachs only, except in the case of EGFR, where expression patterns have not been reported for ZD:WT forestomach/esophagus.

Fig. 2*a* shows that ZS:TG forestomach epithelium was covered by a thin keratin layer and typically showed 2–5 cell thick mucosa with mild folds and basal cell hyperplasia, a phenotype in between that of a ZS:WT and ZD:WT mouse (data not shown; Ref. 32). In stark contrast, ZD:TG epithelium, covered by a thick keratin layer, was very thick with deep mucosal down-growth and severe focal hyperplastic lesions (Fig. 2*b*), greater than that observed in ZD:WT counterparts (data not shown; Ref. 32). Expression of PCNA, an endogenous cell proliferation marker, was mainly in the basal cell layer in ZS:TG forestomach (Fig. 2*c*) but was abundant and detected in many cell layers in the highly hyperplastic ZD:TG epithelium (Fig. 2*d*). As expected, expression of cyclin D1 and its catalytic partner, Cdk4, was strong in both ZS:TG and ZD:TG forestomachs but was scattered in the former (cyclin D1, Fig. 2*e*; Cdk4, Fig. 2*g*) and abundant in many cell layers in the latter (cyclin D1, Fig. 2*f*; Cdk4, Fig. 2*h*). Expression

of p53, a key protein in cell cycle checkpoint, was very weak in ZS:TG (Fig. 2*i*) but moderate and plentiful in ZD:TG forestomach (Fig. 2*j*). Cytoplasmic expression of cytokeratin 14, a biomarker in human (33) and mouse esophageal tumorigenesis (26), although strongly detected in both ZS:TG and ZD:TG forestomach, was restricted to the basal cell layer of the former (ZS:TG, Fig. 2*k*) but present in the many cell layers of the latter (ZD:TG, Fig. 2*l*). In general, the level of expression in each instance was highest in ZD:TG forestomach, followed by ZD:WT and then ZS:TG > ZS:WT.

Aberrant expression and signaling of EGFR contribute to the development of a number of human squamous cell carcinomas, including ESCC (7, 34). Also, EGFR activation is known to drive cell cycle progression in normal and malignant epithelial cells (35, 36). We determined whether such changes occurred in the esophagus and forestomach of ZD:TG and ZD:WT mice in which increased cell proliferation was induced by ZD. Consistent with reports with normal human (37) and mouse esophagus (14), ZS:WT esophagi showed very weak membrane and cytoplasmic staining of EGFR in basal cells (Fig. 3*a*). A slight increase in EGFR expression was detected in the basal cells of ZS:TG esophagi (Fig. 3*c*), consistent with results reported by Mueller *et al.* (14). By contrast, proliferative ZD:WT and ZD:TG esophagi displayed strong EGFR staining in many cell layers, with intensity stronger in ZD:TG (Fig. 3*g*) than ZD:WT (Fig. 3*e*). A similar staining pattern was found in the forestomach: EGFR expression was strong and intense in many cell layers of the proliferative ZD:TG forestomach (Fig. 3*h*), followed by ZD:WT (Fig. 3*f*) and then ZS:TG (Fig. 3*d*) and weakest in ZS:WT forestomach (Fig. 3*b*).

Quantitative PCNA immunohistochemistry revealed that ZD induced a high rate of cell proliferation in the esophagus and forestomach, regardless of cyclin D1 status, relative to their ZS counterparts (Fig. 4). PCNA-LI (%) of cells in S phase, a measure of cellular proliferation, is significantly higher in ZD:WT than ZS:WT tissues (forestomach, 37 ± 2.9 versus 29 ± 2.5 , $P < 0.001$; esophagus, 35 ± 2.7 versus 28 ± 3.4 , $P < 0.01$) and in ZD:TG than ZS:TG tissues (forestomach, 45 ± 7.6 versus 32 ± 4.4 , $P < 0.001$; esophagus, 40 ± 2.2 versus 30 ± 3.7 , $P < 0.01$). In addition, forestomach and esophagus cell proliferation was significantly higher in ZD:TG than ZD:WT mice (forestomach and esophagus, $P < 0.01$, Fig. 4), demonstrating that the highest rate of cell proliferation was achieved when cyclin D1 overexpression in TG mice was combined with ZD.

These data clearly show that cyclin D1 overexpression together with ZD led to the dysregulation of a number of important biomarkers in cell cycle progression and cell differentiation, resulting in robust cell proliferation.

Reduced Apoptosis in Untreated ZD:TG Forestomach. To determine whether apoptosis was reduced in the highly proliferative, untreated ZD:TG forestomach relative to its ZS:TG counterpart, the ApopTag ISOL kit (Serological Corp.) that specifically stains

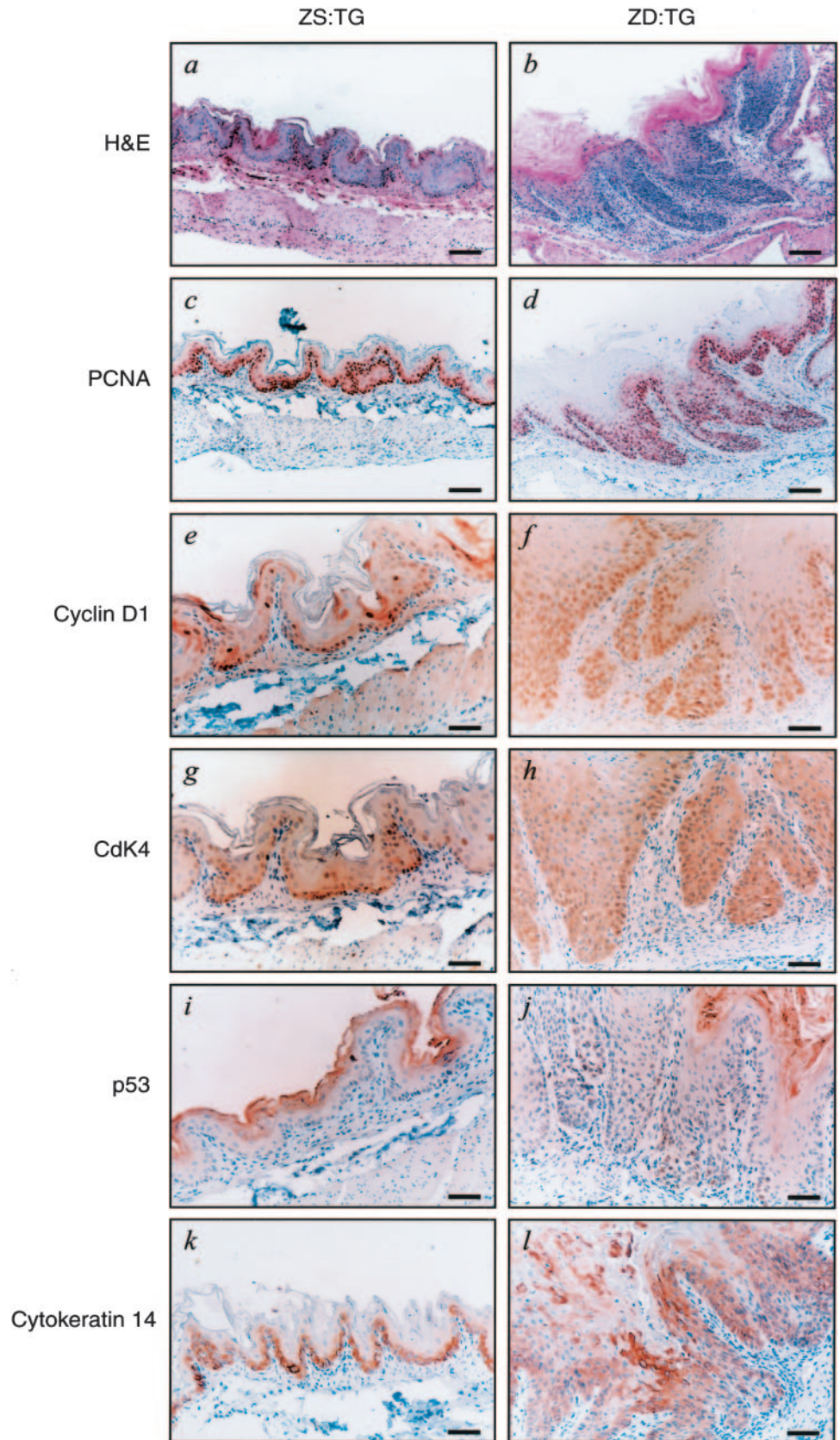


Fig. 2. Forestomach cell proliferation in untreated ZS:TG and ZD:TG mice. H&E staining, immunohistochemistry for PCNA, cyclin D1, Cdk4, p53, and cytokeratin 14 were shown. *Left*, near adjacent forestomach sections from ZS:TG mouse 8; *right*, ZD:TG mouse 1. H&E-stained sections show mild folding in ZS:TG epithelium (*a*) but deep down-growth with focal hyperplastic lesions in ZD:TG epithelium (*b*). PCNA-positive cells, in S phase and G₁-S/G₂ phase, occur mainly in the basal cell layer in ZS:TG epithelium (PCNA, 3-amino-9-ethylcarbazole chromogen, nuclei stained *red*, *c*) but in many cell layers in the proliferative ZD:TG epithelium (*d*). Cyclin D1 is strongly and sparsely detected in ZS:TG epithelium (DAB, nuclei stained *dark brown*, *e*) but abundantly expressed in ZD:TG epithelium (*f*). Cdk4 is weakly detected (DAB, nuclei stained *dark brown*) in ZS:TG epithelium (*g*) but strongly and abundantly expressed in ZD:TG epithelium (*h*). p53-positive nuclei are weak and sparse in ZS:TG forestomach (*i*) but numerous and moderately strong in ZD:TG epithelium (*j*). Cytoplasmic cytokeratin 14 staining is restricted to basal cell layer in ZS:TG forestomach (*k*) but strongly expressed in many cell layers in ZD:TG epithelium (*l*). *a-d*: scale bar = 100 μm. *e-l*: scale bar = 50 μm.

DNA fragmentation or double-strand breaks in apoptotic cells was used. As shown in Fig. 5, ZD:TG epithelium displayed sparse occurrence of ISOL-positive nuclei, mainly in the outermost cell layers (Fig. 5*d*). Conversely, ZS:TG forestomachs regularly

showed ISOL-positive nuclei in basal and suprabasal cell layers, as shown in Fig. 5*a*. Bcl-2, an antiapoptotic protein, was strongly expressed in the proliferative ZD:TG epithelium (Fig. 5*e*) but moderately in ZS:TG epithelium (Fig. 5*b*). On the contrary, Bax, a

EGFR

Esophagus

Forestomach

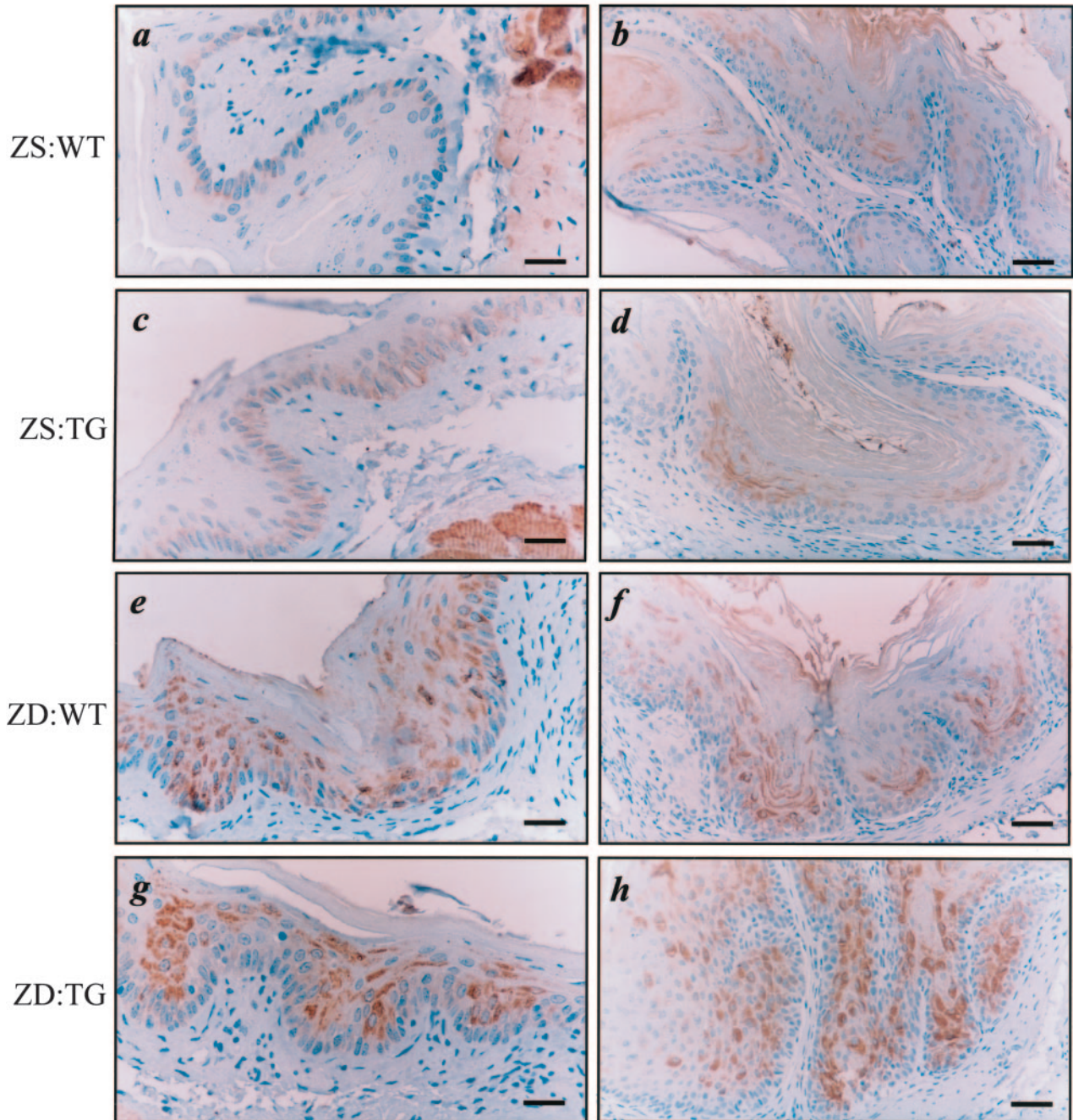


Fig. 3. EGFR expression in untreated ZS:WT, ZD:WT, ZS:TG, and ZD:TG mouse esophagus and forestomach. *Left*: esophagus; *right*: forestomach. ZS:WT mice show weak expression of EGFR (DAB, cytoplasm stained *dark brown*) in the basal cells of esophagus (*a*) and suprabasal cells of forestomach (*b*), whereas ZS:TG mice display moderate staining of EGFR in basal cells and suprabasal cells of esophagus (*c*) and forestomach (*d*). Conversely, ZD:WT mice show strong EGFR expression in the proliferative esophagus (*e*) and forestomach (*f*), whereas ZD:TG mice exhibit very intense and strong EGFR staining in esophagus (*g*) and forestomach (*h*), covering many cell layers. *a, c, e, and g*: scale bar = 25 μm . *b, d, f, and h*: scale bar = 50 μm .

proapoptotic protein, was weakly expressed in the hyperplastic ZD:TG epithelium but moderately in ZS:TG epithelium. A semi-quantitative immunostaining analysis of ZD:TG forestomach produced immunoreactive scores of 3.8 for Bcl-2 and 2.0 for Bax expression, resulting in a Bcl-2/Bax ratio of 1.9 (Table 2). Corresponding ZS:TG forestomach had a score of 2.4 and 2.5 for Bcl-2 and Bax, respectively, producing a Bcl-2:Bax ratio of 1. Thus, an

inverse relationship between Bcl-2 and Bax, favoring cell proliferation, was established in ZD:TG but not in ZS:TG forestomach, a result consistent with the higher proliferative rate observed in the former. Additionally, at 25 days after NMBA treatment, the Bcl-2:Bax ratio was increased ~ 2 -fold in ZD:TG but remained nearly unchanged for ZS:TG forestomach, in line with the high tumor incidence detected in ZD:TG *versus* ZS:TG mice (Table 1).

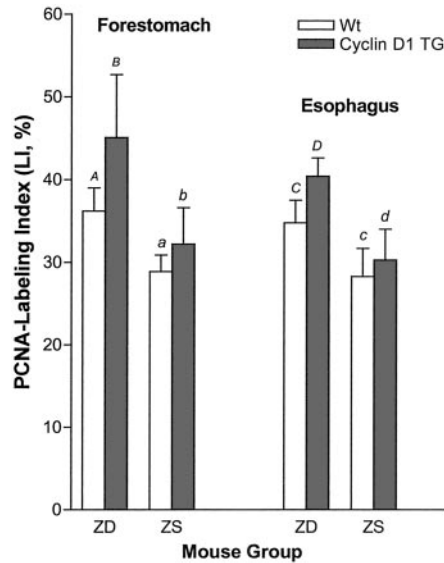


Fig. 4. Rates of cell proliferation in forestomachs and esophagi of untreated ZS:WT, ZD:WT, ZS:TG, and ZD:TG mice. Number of animals (n) for statistical analysis are $n = 5-11$. All statistical tests were two-sided, and error bars are SDs. PCNA-LI (%) is calculated by dividing the number of respective labeled cells in S phase by the total number of cells/cross section of tissue, and the result is expressed as a percentage. Effect of ZD: forestomach, ZD:TG versus ZS:TG, B versus b , $P < 0.001$; ZD:WT versus ZS:WT, A versus a , $P < 0.01$. Esophagus, ZD:TG versus ZS:TG, D versus d , $P < 0.001$; ZD: WT versus ZS: WT, C versus c , $P < 0.01$. Effect of cyclin D1 overexpression: forestomach, ZD:TG versus ZD:WT, B versus A , $P < 0.01$. Esophagus, ZD:TG versus ZD: WT, D versus C , $P < 0.01$.

DISCUSSION

This study showed that collaboration between *cyclin D1* overexpression and ZD resulted in a high rate of cell proliferation in target tissues, setting the stage for rapid carcinogenesis by NMBA. Eighty-six percent of ZD:TG mice developed multiple large or fused tumors in the forestomach after 25 days, with progression to malignancy in 31%. At 77 days, 14% of ZD:TG exhibited small, isolated esophageal papillomas and intestinal metaplasia, a precursor of esophageal ade-

nocarcinoma (Table 1, Fig. 1). Without the added proliferation provided by ZD, the combination of *cyclin D1* overexpression and NMBA was insufficient to initiate esophageal tumorigenesis or mount a vigorous tumorigenic response in the forestomach. The occurrence of forestomach tumors in ZD:TG mice was significantly different from the corresponding ZS:TG group ($P < 0.001$, 25 and 77 days) and from ZD:WT mice ($P = 0.003$, 77 days, Table 1), affirming that collaboration between *cyclin D1* overexpression and ZD are required for rapid tumor initiation by NMBA.

Previous reports of carcinogenesis studies with mice overexpressing *cyclin D1* indicate cellular and tissue context is important. In tissues such as esophagus (15, 38) and skin keratinocytes (39, 40), additional factors are required to promote cancer, whereas in liver (41) and breast (42), *cyclin D1* alone is sufficient to elicit a tumorigenic response. For example, combined *cyclin D1* overexpression and multiple exposures to NMBA resulted only in increased cell proliferation and severity of esophageal and forestomach squamous dysplasia after 15 months, without cancer development (15), whereas cooperation between *cyclin D1* overexpression and *p53* deficiency led to histological evidence of severe oral-esophageal squamous epithelial dysplasia and cancer within 6 months of age (38). Collectively, these studies indicate that the level of *cyclin D1* expression is not a rate-

Table 2 *Bcl-2* and *Bax* protein expression in ZD:TG and ZS:TG mouse forestomachs^a

Diet:genotype (n)	Treatment	Immunoreactive score		
		Bcl-2	Bax	Bcl-2:Bax ratio
ZD:WT (7)	-NMBA	2.9 ± 0.4	2.0 ± 0.7	1.5 ± 0.5
ZS:WT (7)	-NMBA	1.4 ± 0.4	2.9 ± 0.5	0.5 ± 0.2
ZD:TG (7)	-NMBA	3.8 ± 1.1	2.0 ± 0.7	1.9 ± 0.5
ZS:TG (7)	-NMBA	2.4 ± 0.7	2.5 ± 0.4	1.0 ± 0.6
ZD:TG (13)	+NMBA (25 days)	3.9 ± 0.7	1.2 ± 0.4	3.5 ± 1.3
ZS:TG (13)	+NMBA (25 days)	2.7 ± 0.8	2.5 ± 1.1	1.1 ± 0.7

^a Immunoreactive scores = sum of [(grade of percentage of positive cells) × (grade of intensity of staining)] for each component of the forestomach section. n = number of animals. For Bcl-2 expression, ZD:WT versus ZS:WT, $P < 0.01$ (-NMBA); ZD:TG versus ZS:TG, $P < 0.01$ (-NMBA), $P < 0.001$ (+NMBA). For Bax expression, ZD:TG versus ZS:TG (+NMBA), $P < 0.001$. For the Bcl-2/Bax ratio, ZD:WT versus ZS:WT, $P < 0.001$ (-NMBA); ZD:TG versus ZS:TG, $P < 0.01$ (-NMBA), $P < 0.001$ (+NMBA). All statistical tests were two-sided.

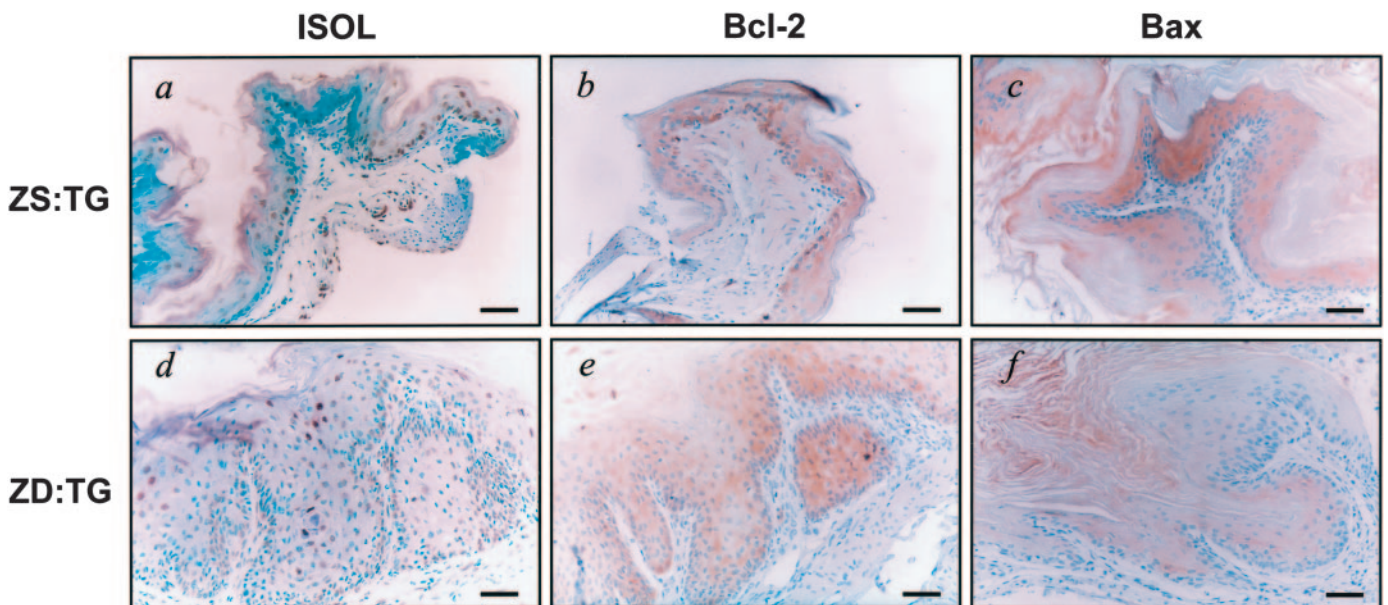


Fig. 5. Apoptosis in forestomachs of untreated ZS:TG and ZD:TG mice. ISOL method, Bcl-2, and Bax immunohistochemical analyses were used. ISOL-positive nuclei (DAB, nuclei stained dark brown) are found in basal and suprabasal cell layers of ZS:TG forestomach (a) but sporadically in outermost cell layer in proliferative ZD:TG forestomach (d). Bcl-2 (DAB, cytoplasm stained brown) is moderately expressed ZS:TG forestomach (b) but strongly and abundantly expressed in ZD:TG forestomach (e). Bax (DAB, cytoplasm stained brown) is moderately expressed in ZS:TG forestomach (c) and weakly and diffusely in ZD:TG forestomach (f). a-f: scale bar = 50 μm.

limiting factor, but rather, for *cyclin D1* overexpression to be tumorigenic, either on its own or in combination with other agents, a high rate of cell proliferation must be sustained (38, 40–42).

This study showed a high rate of forestomach cell proliferation in untreated mice overexpressing *cyclin D1* on a ZD diet, greater than that occurred with either condition alone (Fig. 4). This high rate of proliferation was accompanied by overexpression of several key biomarkers in cell cycle progression (Fig. 2). For example, the hyperplastic ZD:TG epithelium displayed abundant PCNA-positive nuclei in many cell layers concurrently with overexpression of cyclin D1, Cdk4, p53, and cytokeratin 14 (Fig. 2, right panels). Conversely, ZS:TG epithelium with PCNA-positive nuclei limited to basal and directly suprabasal cell layers showed moderate expression of cyclin D1, Cdk4, and cytokeratin 14 but weak expression of p53 in basal cell layers (Fig. 2, left panels). In general, expression of PCNA and that of other biomarkers was greatest in ZD:TG followed by ZD:WT and then ZS:TG>ZS:WT mice, affirming an association between unbridled cell proliferation and deregulation of cell cycle progression.

The EGFR signaling pathway contributes to a number of processes important to tumor development, including cell proliferation, apoptosis, angiogenesis, and metastasis (43). EGFR overexpression occurs frequently in foci of human esophageal squamous dysplasia, a precancerous lesion of ESCC (44) and organotypic culture of primary human esophageal squamous epithelial cells overexpressing EGFR showed epithelial cell proliferation and hyperplasia, with migration of cells from the basal compartment to the suprabasal compartment (45). We have now demonstrated for the first time that the increased cell proliferation induced in esophagus/forestomach by ZD is associated with EGFR overexpression (esophagus, Fig. 3e versus Fig. 3a; forestomach, Fig. 3f versus Fig. 3b), a result that helps to explain the phenomenon of sustained cell expansion in ZD target tissues. Strikingly, ZD mice overexpressing *cyclin D1* exhibited an even more intense and extensive EGFR overexpression than ZD:WT mice, extending from basal to the outermost cell layers of the hyperplastic target tissues (esophagus, Fig. 3g versus Fig. 3e; forestomach, Fig. 3h versus Fig. 3f). By contrast, EGFR staining in ZS:TG tissues was only slightly increased compared with ZS:WT and was confined to basal cell layers (esophagus, Fig. 3c versus Fig. 3a; forestomach, Fig. 3d versus Fig. 3b), consistent with a previous report by Mueller *et al.* (14). Thus, the combination of cyclin D1 overexpression and ZD led to overexpression of EGFR in ZD:TG forestomach, resulting in a hyperplastic and dysplastic microenvironment, conducive to rapid tumor initiation by NMBA. In this regard, EGFR signaling provides a survival signal in murine skin tumor development by activating an antiapoptotic pathway that inhibits keratinocyte differentiation, thereby keeping basal cells in a proliferative state (46).

An antiapoptotic pathway was induced in the proliferative ZD:TG forestomach epithelium. Compared with untreated ZS:TG forestomach, the rate of apoptosis was very low in ZD:TG forestomach. For example, in ZS:TG forestomach, apoptotic cells were regularly found in the basal and suprabasal cell layers (Fig. 5a), whereas in the hyperplastic ZD:TG forestomach epithelium, apoptotic cells were typically scattered and scarce (Fig. 5d), indicating that apoptosis was decreased. Accordingly, the immunoreactive score for Bcl-2, an antiapoptotic protein, was significantly higher in untreated ZD:TG than ZS:TG forestomach (3.8 versus 2.4), whereas that for Bax, a proapoptotic protein, was lower in ZD:TG than ZS:TG forestomach, translating to a high Bcl-2:Bax immunoreactive ratio for ZD:TG forestomach (ZD:TG versus ZS:TG, 1.9 versus 1), favorable to cell proliferation. At 25 days after NMBA treatment, tumor-bearing ZD:TG forestomach showed an additional increase in the Bcl-2:Bax immunoreactive ratio (3.5) whereas that for ZS:TG forestomach remained at the same level as in untreated forestomach. These data point

to a microenvironment in which cell proliferation was preferred via inhibition of apoptosis, providing a platform for rapid tumor initiation by NMBA.

We have, for some time, been developing the mouse model of esophageal/forestomach cancer by manipulating expression of esophageal cancer-relevant proteins such as p53 and Fhit, important in activation of intrinsic apoptotic pathways, so that their loss greatly increased esophageal tumor susceptibility (26, 47).

Absence of the *TP53* tumor suppressor gene rendered ZD mice exquisitely susceptible to NMBA-induced carcinogenesis (26). The rapid rate of tumor induction/progression in ZD:p53^{-/-} mice after a single NMBA dose was accompanied by an increase in the rate of cell proliferation and a decrease in apoptosis. Conversely, overexpression of AZ arrested NMBA-induced forestomach tumorigenesis in ZD mice (32). AZ is a multifunctional regulator of polyamine metabolism that inhibits ornithine decarboxylase activity and restricts polyamine levels (48–50), thereby inhibiting cell proliferation (51). The inhibition of tumor development in ZD mice by AZ overexpression was associated with suppression of cell proliferation and stimulation of apoptosis (32). Thus, in a background of high cellular proliferation provided by ZD that is known to accelerate tumorigenesis, AZ overexpression has the opposite effect of *p53* loss.

It is likely that crossing recombinant mice so that overexpression of cyclin D1, underexpression of p53, and/or Fhit in the same mouse strain, in addition to allowing dissection of pathways to esophageal cancer, will generate a truer model of human esophageal cancer for prevention and therapy studies.

ACKNOWLEDGMENTS

We thank Ben Rhoades (University of Pennsylvania) for maintenance of the TG line, Vu T. Nguyen for technical assistance, and David Super (Thomas Jefferson University, Medical Media Services) for mouse forestomach photography.

REFERENCES

- Doll, R. Geographical variation in cancer incidence: a clue to causation. *World J. Surg.*, 2: 595–602, 1978.
- Joint Iran-International Agency for Research on Cancer Study Group. Esophageal cancer studies in the Caspian littoral of Iran: results of population studies-A pro-drome. *J. Natl. Cancer Inst. (Bethesda)*, 59: 1127–1138, 1978.
- Yang, C. S. Research on esophageal cancer in China. *Cancer Res.*, 40: 2633–2644, 1980.
- van Rensburg, S. J. Epidemiologic and dietary evidence for a specific nutritional predisposition to esophageal cancer. *J. Natl. Cancer Inst. (Bethesda)*, 67: 243–251, 1981.
- Lu, S. H., Montesano, R., Zhang, M. S., Feng, L., Luo, F. J., Chui, S. X., Umbenhauer, D., Saffhill, R., and Rajewsky, M. F. Relevance of *N*-nitrosamines to esophageal cancer in China. *J. Cell. Physiol. Suppl.*, 4: 51–58, 1986.
- Lu, S. H., Chui, S. X., Yang, W. X., Hu, X. N., Guo, L. P., and Li, F. M. Relevance of *N*-nitrosamines to esophageal cancer in China. *IARC Scientific Publ. No. 105*, pp. 11–17. Lyon, France: IARC Scientific Publications, 1991.
- Mandard, A. M., Hainaut, P., and Hollstein, M. Genetic steps in the development of squamous cell carcinoma of the esophagus (Review). *Mutat. Res.*, 462: 335–342, 2000.
- Jiang, W., Kahn, S. M., Tomita, N., Zhang, Y. J., Lu, S. H., and Weinstein, I. B. Amplification and expression of the human *cyclin D* gene in esophageal cancer. *Cancer Res.*, 152: 2980–2983, 1992.
- Jiang, W., Zhang, Y. J., Kahn, S. M., Hollstein, M. C., Santella, R. M., Lu, S. H., Harris, C. C., Montesano, R., and Weinstein, I. B. Altered expression of the *cyclin D1* and *retinoblastoma* genes in human esophageal cancer. *Proc. Natl. Acad. Sci. USA*, 90: 9026–9030, 1993.
- Arber, N., Lightdale, C., Rotterdam, H., Han, K. H., Sgambato, A., Yap, E., Ahsan, H., Finegold, J., Stevens, P. D., Green, P. H., Hibshoosh, H., Neugut, A. I., Holt, P. R., and Weinstein, I. B. Increased expression of the *cyclin D1* gene in Barrett's esophagus. *Cancer Epidemiol. Biomark. Prev.*, 5: 457–459, 1996.
- Wang, Q. S., Sabourin, C. L., Wang, H., and Stoner, G. D. Overexpression of cyclin D1 and cyclin E in *N*-nitrosomethylbenzylamine-induced rat esophageal tumorigenesis. *Carcinogenesis (Lond.)*, 17: 1583–1588, 1996.
- Youssef, E. M., Hasuma, T., Morishima, Y., Takada, N., Osugi, H., Higashino, M., Otani, S., and Fukushima, S. Overexpression of cyclin D1 in rat esophageal carcinogenesis model. *Jpn. J. Cancer Res.*, 88: 18–25, 1997.

13. Nakagawa, H., Wang, T. C., Zukerberg, L., Odze, R., Togawa, K., May, G. H., Wilson, J., and Rustgi, A. K. The targeting of the cyclin D1 oncogene by an Epstein-Barr virus promoter in transgenic mice causes dysplasia in the tongue, esophagus and forestomach. *Oncogene*, *14*: 1185–1190, 1997.
14. Mueller, A., Odze, R., Jenkins, T. D., Shahsafaie, A., Nakagawa, H., Inomoto, T., and Rustgi, A. K. A transgenic mouse model with cyclin D1 overexpression results in cell cycle, epidermal growth factor receptor, and p53 abnormalities. *Cancer Res.*, *57*: 5542–5549, 1997.
15. Jenkins, T. D., Mueller, A., Odze, R., Shahsafaie, A., Zukerberg, L. R., Kent, R., Stoner, G. D., and Rustgi, A. K. Cyclin D1 overexpression combined with *N*-nitrosomethylbenzylamine increases dysplasia and cellular proliferation in murine esophageal squamous epithelium. *Oncogene*, *18*: 59–66, 1999.
16. Magee, P. N. The experimental basis for the role of nitroso compounds in human cancer. *Cancer Surv.*, *8*: 207–239, 1989.
17. Fong, L. Y. Y., Sivak, A., and Newberne, P. M. Zinc deficiency and methylbenzyl-nitrosamine induced esophageal cancer in rats. *J. Natl. Cancer Inst. (Bethesda)*, *61*: 145–150, 1978.
18. Fong, L. Y. Y., Li, J. X., Farber, J., and Magee, P. N. Cell proliferation and esophageal tumorigenesis in the zinc deficient rat. *Carcinogenesis (Lond.)*, *17*: 1841–1848, 1996.
19. Fong, L. Y. Y., Lau, K. M., Huebner, K., and Magee, P. N. Induction of esophageal tumors in zinc-deficient rats by single low doses of *N*-nitrosomethylbenzylamine (NMBA): analysis of cell proliferation, and mutations in *H-ras* and *p53* genes. *Carcinogenesis (Lond.)*, *18*: 1477–1484, 1997.
20. Fong, L. Y. Y., Nguyen, V. T., Farber, J. L., Huebner, K., and Magee, P. N. Early deregulation of the p16^{ink4a}-cyclin D1/Cdk4-Rb pathway in cell proliferation-driven esophageal tumorigenesis in zinc-deficient rats. *Cancer Res.*, *60*: 4589–4595, 2000.
21. Fong, L. Y. Y., Pegg, A. E., and Magee, P. N. α -Difluoromethylornithine inhibits *N*-nitrosomethylbenzylamine-induced esophageal carcinogenesis in zinc-deficient rats: effects on esophageal cell proliferation and apoptosis. *Cancer Res.*, *58*: 5380–5388, 1998.
22. Fong, L. Y. Y., Nguyen, V. T., Pegg, A. E., and Magee, P. N. α -Difluoromethylornithine induction of apoptosis: a mechanism which reverses pre-established cell proliferation and cancer initiation in esophageal carcinogenesis in zinc-deficient rats. *Cancer Epidemiol. Biomark. Prev.*, *10*: 189–198, 2001.
23. Fong, L. Y. Y., Nguyen, V. T., and Farber, J. L. Esophageal cancer prevention in zinc-deficient rats: rapid induction of apoptosis by zinc replenishment. *J. Natl. Cancer Inst. (Bethesda)*, *93*: 1525–1533, 2001.
24. Siglin, J. C., Khare, L., and Stoner, G. D. Evaluation of dose and treatment duration on the esophageal tumorigenicity of *N*-nitrosomethylbenzylamine in rats. *Carcinogenesis (Lond.)*, *16*: 259–265, 1995.
25. Fong, L. Y. Y., and Magee, P. N. Dietary zinc deficiency enhances esophageal cell proliferation and *N*-nitrosomethylbenzylamine (NMBA)-induced esophageal tumor incidence in C57BL/6 mouse. *Cancer Lett.*, *143*: 63–69, 1999.
26. Fong, L. Y. Y., Ishii, H., Nguyen, V. T., Vecchione, A., Farber, J. L., Croce, C. M., and Huebner, K. p53 deficiency accelerates induction and progression of esophageal and forestomach tumors in zinc-deficient mice. *Cancer Res.*, *63*: 186–195, 2003.
27. Krajewska, M., Krajewski, S., Epstein, J. I., Shabaik, A., Sauvageot, J., Song, K., and Kitada, S., and Reed, J. C. Immunohistochemical analysis of bcl-2, bax, bcl-X and mcl-1 expression in prostate cancers. *Am. J. Pathol.*, *148*: 1567–1576, 1996.
28. Didenko, V. V. Detection of specific double-strand DNA breaks and apoptosis *in situ* using T4 DNA ligase. *Methods Mol. Biol.*, *203*: 143–151, 2002.
29. Didenko, V. V., Tunstead, J. R., and Hornsby, P. J. Biotin-labeled hairpin oligonucleotides: probes to detect double-strand breaks in DNA in apoptotic cells. *Am. J. Pathol.*, *152*: 897–902, 1998.
30. The GLM procedure. SAS/STAT User's Guide, Ed. 4, Vol. 2. Cary, NC: SAS Institute, Inc., 1989.
31. Armitage, P., and Berry, G. *Statistical Methods in Medical Research*. Oxford, United Kingdom: Blackwell Scientific Publications, 1987.
32. Fong, L. Y. Y., Feith, D. J., and Pegg, A. E. Antizyme overexpression in transgenic mice reduces cell proliferation and *N*-nitrosomethylbenzylamine-induced forestomach carcinogenesis. *Cancer Res.*, *63*: 3945–3954, 2003.
33. Cintonio, M., Tripod, S. A., Santopietro, R., Antonio, P., Lutfi, A., Chang, F., Syrjanen, S., Shen, Q., Tosi, P., and Syrjanen, K. Cytokeratin expression patterns as an indicator of tumour progression in oesophageal squamous cell carcinoma. *Anticancer Res.*, *21*: 4195–4201, 2001.
34. Hollstein, M. C., Smits, A. M., Galiana, C., Yamasaki, H., Bos, J. L., Mandard, A., Partensky, C., and Montesano, R. Amplification of epidermal growth factor receptor gene but no evidence of ras mutations in primary human esophageal cancers. *Cancer Res.*, *48*: 5119–5123, 1988.
35. Vardy, D. A., Kari, C., Lazarus, G. S., Jensen, P. J., Zilberstein, A., Plowman, G. D., and Rodeck, U. Induction of autocrine epidermal growth factor receptor ligands in human keratinocytes by insulin/insulin-like growth factor-1. *J. Cell. Physiol.*, *163*: 257–265, 1995.
36. Huang, S. M., Bock, J. M., and Harari, P. M. Epidermal growth factor receptor blockade with C225 modulates proliferation, apoptosis, and radiosensitivity in squamous cell carcinomas of the head and neck. *Cancer Res.*, *59*: 1935–1940, 1999.
37. Calabro, A., Orsini, B., Renzi, D., Papi, L., Surrenti, E., Amorosi, A., Herbst, H., Milani, S., and Surrenti, C. Expression of epidermal growth factor, transforming growth factor α and their receptor in the human oesophagus. *Histochem. J.*, *29*: 745–758, 1997.
38. Opitz, O. G., Harada, H., Suliman, Y., Rhoades, B., Sharpless, N. E., Kent, R., Kopelovich, L., Nakagawa, H., and Rustgi, A. K. A mouse model of human oral-esophageal cancer. *J. Clin. Invest.*, *110*: 761–769, 2002.
39. Rodriguez-Puebla, M. L., LaCava, M., and Conti, C. J. Cyclin D1 overexpression in mouse epidermis increases cyclin-dependent kinase activity and cell proliferation *in vivo* but does not affect skin tumor development. *Cell Growth Differ.*, *10*: 467–472, 1999.
40. Yamamoto, H., Ochiya, T., Takeshita, F., Toriyama-Baba, H., Hirai, K., Sasaki, H., Sasaki, H., Sakamoto, H., Yoshida, T., Saito, I., and Terada, M. Enhanced skin carcinogenesis in cyclin D1-conditional transgenic mice: cyclin D1 alters keratinocyte response to calcium-induced terminal differentiation. *Cancer Res.*, *62*: 1641–1647, 2002.
41. Deane, N. G., Parker, M. A., Aramandla, R., Diehl, L., Lee, W. J., Washington, M. K., Nanney, L. B., Shyr, Y., and Beauchamp, R. D. Hepatocellular carcinoma results from chronic cyclin D1 overexpression in transgenic mice. *Cancer Res.*, *61*: 5389–5395, 2001.
42. Wang, T. C., Cardiff, R. D., Zukerberg, L., Lees, E., Arnold, A., and Schmidt, E. V. Mammary hyperplasia and carcinoma in MMTV-cyclin D1 transgenic mice. *Nature (Lond.)*, *369*: 669–671, 1994.
43. Schlessinger, J. Cell signaling by receptor tyrosine kinases. *Cell*, *103*: 211–225, 2000.
44. Itakura, Y., Sasano, H., Shiga, C., Furukawa, Y., Shiga, K., Mori, S., and Nagura, H. Epidermal growth factor receptor overexpression in esophageal carcinoma. An immunohistochemical study correlated with clinicopathologic findings and DNA amplification. *Cancer (Phila.)*, *74*: 795–804, 1994.
45. Andl, C. D., Mizushima, T., Nakagawa, H., Oyama, K., Harada, H., Chruma, K., Herlyn, M., and Rustgi, A. K. Epidermal growth factor receptor mediates increased cell proliferation, migration, and aggregation in esophageal keratinocytes *in vitro* and *in vivo*. *J. Biol. Chem.*, *278*: 1824–1830, 2003.
46. Sibilina, M., Fleischmann, A., Behrens, A., Stingl, L., Carroll, J., Watt, F. M., Schlessinger, J., and Wagner, E. F. The EGF receptor provides an essential survival signal for SOS-dependent skin tumor development. *Cell*, *102*: 211–220, 2000.
47. Dumon, K. R., Ishii, H., Fong, L. Y. Y., Zanasi, N., Fidanza, V., Vecchione, A., Baffa, R., Trapasso, F., During, M. J., Huebner, K., and Croce, C. M. *FHIT* gene therapy prevents tumor development in Fhit deficient mice. *Proc. Natl. Acad. Sci. USA*, *98*: 3346–3351, 2001.
48. Hayashi, S., Murakami, Y., and Matsufuji, S. Ornithine decarboxylase antizyme: a novel type of regulatory protein. *Trends Biochem. Sci.*, *21*: 27–30, 1996.
49. Coffino, P. Regulation of cellular polyamines by antizyme. *Nat. Rev. Mol. Cell. Biol.*, *2*: 188–194, 2001.
50. Feith, D. J., Shantz, L. M., and Pegg, A. E. Targeted antizyme expression in the skin of transgenic mice reduces tumor promoter induction of ornithine decarboxylase and decreases sensitivity to chemical carcinogenesis. *Cancer Res.*, *61*: 6073–6081, 2001.
51. Mitchell, J. L., Leyser, A., Holtorff, M. S., Bates, J. S., Frydman, B., Valasinas, A., Reddy, V. K., and Marton, L. J. Antizyme induction by polyamine analogues as a factor of cell growth inhibition. *Biochem. J.*, *366*: 663–671, 2002.